Direct Measurement of the Rate Coefficient for the CH_2═$C(CH_3)C(O)O_2$ + NO Reaction Using Chemical Ionization Mass Spectrometry

Joost A. de Gouw[†] **and Carleton J. Howard***

Aeronomy Laboratory, NOAA, Environmental Research Laboratories, Boulder, Colorado 80303

Received: June 30, 1997; In Final Form: September 15, 1997[⊗]

In the troposphere, the CH_2═$C(CH_3)C(O)O_2$, or peroxymethacryl, radical is formed as an intermediate in the photooxidation of isoprene, one of the most important biogenic hydrocarbons in the atmosphere. The reaction between CH_2═$C(CH_3)C(O)O_2$ and NO produces NO_2 and subsequently ozone. The rate coefficient for the CH_2═$C(CH_3)C(O)O_2$ + NO reaction is measured directly over the temperature range 240−360 K and at pressures of 1.3−3.9 Torr using a flow tube reactor and chemical ionization mass spectrometry detection. The results are given by $k(T) = 8.7 \times 10^{-12} \exp(290/T)$ cm^3 molecule^{-1} s^{-1}, accurate within ±20% over the 240−360 K range, with a value at 298 K of $(2.3 \pm 0.3) \times 10^{-11}$ cm^3 molecule^{-1} s^{-1}. These results agree within the experimental uncertainties with the measured results for the analogous $CH_3C(O)O_2$ + NO reaction, suggesting that the rate coefficient for $RC(O)O_2$ + NO reactions may not be sensitive to the structure of the R group. Only NO_2 could be positively identified as a reaction product.

1. Introduction

Isoprene (2-methyl-1,3-butadiene) is one of the most important biogenic hydrocarbons in the atmosphere: it is emitted in large quantities by certain types of vegetation,[1] notably deciduous trees, and is readily oxidized by OH, O_3, and NO_3.[2,3] In polluted air, the photooxidation of isoprene contributes to the production of ozone,[4] one of the key constituents of photochemical smog. To estimate the relative roles played by anthropogenic (AHC) and biogenic hydrocarbon (BHC) emissions in tropospheric ozone formation, an understanding of the atmospheric chemistry of isoprene is of key importance.

The photooxidation mechanism of isoprene is complex and has been described by Paulson and Seinfeld[2] and, more recently, by Carter and Atkinson.[3] Under most conditions, isoprene reacts primarily with OH to form methacrolein (CH_2═$C(CH_3)CHO$; branching ratio 25%), methyl vinyl ketone ($CH_3COCHCH_2$; branching ratio 36%), and a number of other minor species.[5] Further photooxidation of methacrolein by OH leads in about 50% of the cases to the formation of the CH_2═$C(CH_3)C(O)O_2$ (peroxymethacryl or PMA) radical,[6] which reacts predominantly with NO and NO_2:

$$CH_2{=}C(CH_3)C(O)O_2 + NO \rightarrow CH_2{=}C(CH_3)C(O)O + NO_2 \quad (1)$$

$$CH_2{=}C(CH_3)C(O)O_2 + NO_2 \underset{\Delta}{\overset{M}{\rightleftharpoons}} CH_2{=}C(CH_3)C(O)O_2NO_2 \quad (2, -2)$$

The formation of NO_2 through reaction 1 rapidly leads to the production of ozone:

$$NO_2 + h\nu\ (\lambda < 380\ \text{nm}) \rightarrow NO + O \quad (3)$$

$$O + O_2 \xrightarrow{M} O_3 \quad (4)$$

Reactions 3 and 4 are fast under atmospheric conditions, causing reaction 1 to be the rate-limiting step in the production of ozone. The product of reaction 2, CH_2═$C(CH_3)C(O)O_2NO_2$ (alternatively referred to as peroxymethacrylic nitric anhydride or MPAN and peroxymethacryloyl nitrate or PMN), is relatively stable and acts therefore as a reservoir species for NO_2. A major sink of MPAN in the atmosphere is thermal decomposition into NO_2 and the CH_2═$C(CH_3)C(O)O_2$ radical, i.e., the reverse reaction −2, thus providing a mechanism for NO_2 transport into less polluted regions.

The presence of MPAN in the atmosphere is almost entirely the result of BHC emissions. Recent airborne measurements of MPAN by Williams et al.[7] over the central and southeastern U.S. suggest that the observed MPAN concentrations can be used as a parameter to quantify the effect of BHC emissions on ozone levels. It is clear that further verification of this important result requires a detailed knowledge of the atmospheric chemistry of MPAN. Thermal decomposition of MPAN, which has been studied by Roberts and Bertman,[8] and the subsequent PMA + NO reaction 1 are an important sink for MPAN. A detailed knowledge of the rates of these processes and the products formed is essential in the interpretation of observed tropospheric MPAN levels.

It is the purpose of the present work to measure the rate coefficient for reaction 1 using chemical ionization mass spectrometry (CIMS) over a wide range of temperatures. At present, there have been no reported measurements of the rate coefficient for this reaction. The analogue of reaction 1 in the case of PAN ($CH_3C(O)O_2NO_2$ or peroxyacetyl nitrate), i.e., $CH_3C(O)O_2$ + NO, has been studied by, among other workers, Maricq and Szente[9] and in this laboratory by Villalta and Howard.[10] The products of reaction 1 are presently unknown, and a product study using CIMS is undertaken. By analogy with the $CH_3C(O)O_2$ + NO reaction, it is expected that the product of reaction 1, CH_2═$C(CH_3)C(O)O$, decomposes into the methylvinyl radical, CH_2═$C-CH_3$, and CO_2.

2. Experimental Section

The experiments are performed using chemical ionization mass spectrometry (CIMS). The setup consists of (1) a source of CH_2═$C(CH_3)C(O)O_2$ radicals, (2) a neutral flow tube reactor, in which the reaction with NO takes place, (3) an ion flow tube, in which the neutral species from the neutral reactor undergo

[†] Cooperative Institute for Research in Environmental Sciences, University of Colorado, Boulder, Colorado 80309.

[⊗] Abstract published in *Advance ACS Abstracts,* October 15, 1997.

S1089-5639(97)02107-5 CCC: $14.00

specific ion−molecule reactions, and (4) a mass spectrometer to determine the mass and intensities of the resulting ions. The setup has been described in detail before,[11] and only a brief description is given here.

The CH_2═$C(CH_3)C(O)O_2$, or PMA, radicals are generated by flowing MPAN vapor in He through a 10 cm long × 0.9 cm i.d. quartz tube heated to 190−210 °C. The MPAN is synthesized using the method outlined by Bertman and Roberts[12] and stored in tridecane. When not in use, the sample is stored in contact with dry ice. Besides tridecane and MPAN, the sample contains some methacrylic anhydride, $[CH_2$═$C(CH_3)CO]_2O$, which is used in the synthesis. Neither the tridecane nor the methacrylic anhydride interferes with the present experiments, because the PMA radical is detected directly. When producing radicals, the sample is kept in a water/ice bath, and a small flow (0.1−1.0 STP cm^3 s^{-1}) of He (>99.9995%) is bubbled through the liquid. A larger flow of He (9.0−12.0 STP cm^3 s^{-1}) is added downstream of the MPAN sample but upstream of the heated quartz tube. Both the temperature and the He flow through the quartz tube are chosen to optimize the radical yield; the pressure is roughly the same as in the neutral flow tube. At these source conditions, the residence time of MPAN in the quartz tube is about 10^{-3} s. Using the reported rate coefficient for thermal decomposition of MPAN,[8] the dissociation of MPAN is estimated to be almost complete in the radical source. If the temperature of the quartz tube is too high, the radical concentration decreases, possibly due to radical−radical reactions, thermal decomposition of the radicals, or increased wall losses inside the quartz tube.

The neutral flow tube reactor consists of a 120 cm long × 2.54 cm i.d. Pyrex tube. The temperature in the last 60 cm of the flow reactor can be controlled. The He flow containing the radicals is introduced to the neutral flow reactor a few centimeters upstream of the temperature-regulated reaction zone. The balance of the He carrier gas is added to the flow tube upstream of the radical inlet. The neutral flow reactor is coupled to the ion flow tube through a throttle valve, which is used to regulate the pressure (1.3−3.9 Torr) and the average flow velocity (1200−1700 cm s^{-1}) of the He carrier gas inside the neutral flow reactor. For the measurements at low temperatures, a 2.23 cm i.d. Teflon tube is inserted in the neutral flow reactor to reduce the wall loss of radicals and thus increase the radical signal.

Small flows of NO gas (1.5×10^{-4}−5.2×10^{-3} STP cm^3 s^{-1}) are introduced to the flow reactor through a 120 cm long × 0.64 cm o.d. Pyrex inlet tube, which can be moved along the center of the flow reactor. By moving the inlet, the reaction time between the PMA radicals and NO is varied, which is how rate coefficients are determined using the present technique. The NO gas (>99.0%) is passed through a dry ice-cooled silica gel trap, prior to the flow reactor, to reduce the amount of NO_2 impurity present. The residual NO_2 in the NO gas is estimated using CIMS detection of NO_2 with SF_6^- to be less than 0.1% of the NO concentration. The association reaction 2 between PMA radicals and NO_2 is expected to be somewhat slower than reaction 1.[13] At these small NO_2 concentrations, the rate of reaction 2 is negligible and cannot interfere with the measurement of the rate coefficient of reaction 1. The NO flow rates are measured by flowing the NO into a calibrated volume and by measuring the rate of pressure increase.

A large flow (90−105 STP cm^3 s^{-1}) of He (>99.5%) is pumped through the 130 cm × 7.30 cm i.d. ion flow tube by a 500 L s^{-1} mechanical booster pump, resulting in a pressure of 0.5−0.6 Torr and an average flow velocity of 3000−4000 cm s^{-1}. Ions are produced at the upstream end of the flow tube in an electron-impact source. Trace amounts of SF_6, CF_3I, or O_2 are added just upstream of the ion source to produce SF_6^-, I^-, and O_2^+ ions, respectively. A pinhole at the end of the flow tube samples a portion of the ions in the buffer gas, and a quadrupole mass spectrometer, mounted behind the pinhole, is used to identify the ions and monitor their intensities.

The neutral flow reactor is coupled to the ion flow tube 50 cm upstream of the pinhole. CIMS detection of the reagents or products of a reaction is accomplished through ionization by a specific reagent ion. Based on the detection of the $CH_3C(O)O_2$ radicals by Villalta and Howard,[10] the following ion−molecule reaction is expected to enable the detection of PMA radicals:

$$CH_2\text{═}C(CH_3)C(O)O_2 + SF_6^- \rightarrow CH_2\text{═}C(CH_3)C(O)O_2^- + SF_6 \quad (5)$$

The rate equation for reaction 5 is given by

$$d[PMA^-]/dt = k_{ion}[SF_6^-][PMA] \quad (6)$$

where k_{ion} is the rate coefficient for this reaction. If only a small fraction of the SF_6^- ions react with the gas from the neutral reactor, including the PMA radicals, eq 6 can be approximated by

$$[PMA^-] = k_{ion}[SF_6^-][PMA]\Delta t \quad (7)$$

in which Δt is the total ion−neutral reaction time. Since k_{ion}, $[SF_6^-]$, and Δt are constants, it can be seen from eq 7 that the signal of CH_2═$C(CH_3)C(O)O_2^-$ ions is proportional to the corresponding radical concentration.

3. Results

Detection of CH_2═$C(CH_3)C(O)O_2$, or PMA, radicals is found to be possible using SF_6^- ions. When the temperature of the quartz tube in the radical source is increased, an ion signal at the expected mass, 101 amu, is seen. Furthermore, NO_2, produced by reaction −2, is also detected as NO_2^- using SF_6^-, and the corresponding signal depends similarly on the quartz tube temperature. When NO is added to the neutral flow reactor, the PMA signal decreases and the NO_2 signal increases as a result of reaction 1. PMA radicals could also be detected as CH_2═$C(CH_3)C(O)O^-$ using I^- ions, but in this case the background signal was too high for accurate rate coefficient measurements. The background is defined as the signal at mass 101 (or mass 85 in the case of I^-) with either the radical source turned off or all the PMA radicals being depleted in the asymptotic limit of high NO concentrations. In case of SF_6^-, the background is typically 50−100 counts s^{-1}. The concentration of PMA radicals is estimated using the observed concentration of NO_2. In the absence of NO a typical value of 1.4×10^{11} molecules cm^{-3} is obtained. The numbers used to find this value are the measured signals of NO_2^- (10^4 counts s^{-1}) and SF_6^- (10^6 counts s^{-1}), the calculated reaction time Δt between SF_6^- and NO_2 (14×10^{-3} s), and the rate coefficient for the charge-transfer reaction between SF_6^- and NO_2 (1.4×10^{-10} cm^3 $molecule^{-1}$ s^{-1}).[14] At these radical concentrations, radical−radical reactions are expected to be of minor importance.[15]

A typical result of a kinetics measurement using SF_6^- detection is shown in Figure 1, in which the CH_2═$C(CH_3)C(O)O_2^-$ ion signal, corresponding to the concentration of PMA radicals, is shown as a function of the NO inlet position, at various NO flow rates. The resulting NO concentrations are

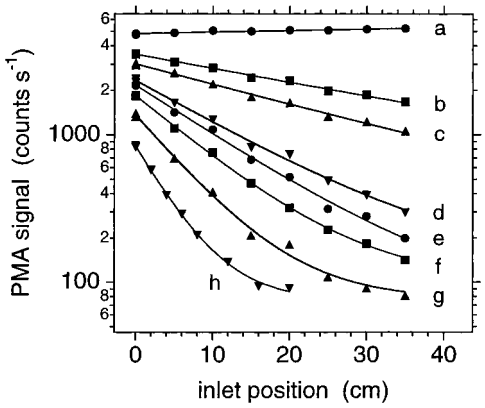

Figure 1. Ion signal corresponding to the concentration of $CH_2{=}C(CH_3)C(O)O_2$, or PMA, radicals as a function of the position of the NO inlet, for eight different NO concentrations: (a) 0, (b) 1.39×10^{12}, (c) 2.19×10^{12}, (d) 5.08×10^{12}, (e) 6.24×10^{12}, (f) 7.37×10^{12}, (g) 1.01×10^{13}, and (h) 1.65×10^{13} molecules cm^{-3}. The symbols represent the experimental data, whereas the solid curves show the results of fitting an exponential function to the data. The data are taken at a temperature of 302 K, a pressure of 1.93 Torr, a He flow of 15.1 STP cm^3 s^{-1}, and an average flow velocity of 1680 cm s^{-1}.

chosen to be much higher (at least 10 times) than the concentration of PMA radicals, which is sufficient to ensure pseudo-first-order reaction conditions. In this case the dependence of the PMA signal S_{PMA} on the reaction length z is given by

$$S_{PMA} = (S_{PMA,z=0} - B) \exp(-k_m z/v) + B \qquad (8)$$

where k_m is the measured first-order rate coefficient (s^{-1}), v the average flow velocity (cm s^{-1}), and B the background signal. Values of k_m are determined from the measurements as in Figure 1 by fitting eq 8 to the data. The curvature in the measurements at high NO concentrations is due to the nonzero background B. In principle, each of the k_m values as determined from the measurements results in a value for the rate coefficient k for reaction 1. However, the loss of radicals on the wall of the movable inlet also depends on the inlet position and has to be taken into account. The measured rate coefficient k_m can be given as

$$k_m = k[NO] - k_w \qquad (9)$$

where [NO] is the NO concentration and k_w the first-order rate coefficient for the loss of PMA radicals on the wall of the movable injector. The injector wall loss of PMA radicals is opposite in sign to the reactive loss, because the amount of injector surface exposed to the radical stream decreases as the injector is withdrawn and the reaction time increases. The value of k_w can be experimentally determined by performing a measurement at zero NO concentration and is typically quite small (3 s^{-1} on average), except at lower temperatures, where it tends to increase. To account for wall loss, the rate coefficient k_m is measured at a number of NO concentrations (Figure 1). The resulting values for k_m are plotted versus [NO] as in Figure 2. Equation 9 is fit to the data in Figure 2, resulting in a value for k from the slope and for k_w from the intercept at [NO] = 0. The injector wall loss is not to be confused with the loss of radicals on the wall of the neutral flow reactor. Since the radical inlet is fixed, the stream of radicals is always exposed to the same amount of reactor wall. Therefore, the first-order reactor wall loss provides an additional loss of radicals, but the loss is independent of the NO injector position and does not have to be taken into account in the analysis of the measurements.

The reaction between $CH_2{=}C(CH_3)C(O)O_2$ radicals and NO is studied at temperatures ranging from 240 to 360 K. The

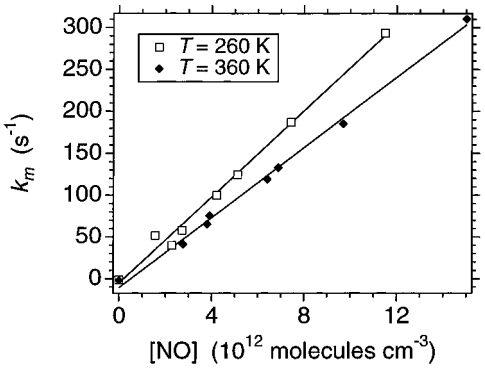

Figure 2. Measured rate coefficients k_m vs the NO concentration at 260 and 360 K. The rate coefficient k for the $CH_2{=}C(CH_3)C(O)O_2$ + NO reaction is determined from a fit of a linear function to the data.

results are given in Table 1 and shown in an Arrhenius plot in Figure 3. All the measurements were done with SF_6^- as a reagent ion; using I^- the background is too high to obtain accurate data. Some of the measurements are taken with a Teflon tube inserted in the neutral flow reactor (see Table 1) to reduce the reactor wall loss of PMA radicals. The minimum temperature at which the experiment is still feasible is about 20 K lower when using the Teflon tube. From Table 1 and Figure 3 it can be seen that the measurements with and without Teflon agree well. The different wall material and flow conditions (the Teflon tube has a smaller diameter) do not influence the experimental results, indicating the absence of interference from wall reactions. Also, the measurements at 330 K are performed at three different He pressures, to rule out any pressure dependence of the final result. The line in Figure 3 shows the result of a fit of the function $k(T) = A \exp(-E_a/RT)$ to the data. All data points are taken with equal weights. From the fit, it is found that $A = (8.7 \pm 2.3) \times 10^{-12}$ cm^3 molecule^{-1} s^{-1} and $E_a/R = -(290 \pm 70)$ K, where the error bars represent the 95% confidence level. A value of $(8.7 \pm 3.2) \times 10^{-12}$ cm^3 molecule^{-1} s^{-1} is recommended for the preexponential factor A, to account for a 10% possible systematic error. The relatively large uncertainty in A arises from the fact that this value is extrapolated from the data to $T = \infty$. Over the temperature range 240−360 K, covered in the experiments, the expression $k(T) = 8.7 \times 10^{-12} \exp(290/T)$ cm^3 molecule^{-1} s^{-1} is estimated to be accurate within ±20%, including a factor of 10% for possible systematic error.

At flow reactor temperatures higher than 360 K, some of the MPAN, which is not dissociated in the heated quartz tube, is dissociated inside the neutral flow reactor. This provides an additional source of PMA radicals in the reaction zone and seriously compromises the kinetic measurements. In principle, the MPAN can be 100% dissociated inside the radical source, by heating the quartz tube to higher temperatures. Unfortunately, this also reduces the PMA radical yield to impractical values, possibly as a result of increased wall losses inside the quartz tube, further thermal decomposition of the radical, or radical−radical reactions such as[16]

$$2CH_2{=}C(CH_3)C(O)O_2 \rightarrow 2CH_2{=}C(CH_3)C(O)O + O_2 \qquad (10)$$

which could start to play a role if the radical concentration increases at higher temperatures. At flow reactor temperatures lower than 240 K, the PMA signal is too small for an accurate rate coefficient measurement, probably because the reactor wall loss of radicals is too high. At 220 K, the PMA signal is reduced to about 5% of its room-temperature value. This suggests that the reactor wall loss is about 60 s^{-1}, assuming that wall loss is small at room temperature as observed for other

TABLE 1: Experimental Results for the Rate Coefficient *k* of the CH_2=$C(CH_3)C(o)O_2$ + NO Reaction[a]

T (K)	Teflon tube	*p* (Torr)	He flow (STP cm^3 s^{-1})	velocity (cm s^{-1})	no. of expts	[NO] range (10^{12} molecules cm^{-3})	*k* (10^{-11} cm^3 $molecule^{-1}$ s^{-1})
240	yes	2.01	15.0	1280	9	0.8−6.7	3.09 ± 0.18
240	yes	1.91	15.1	1350	9	2.2−16.2	2.66 ± 0.17
260	yes	2.03	15.0	1380	8	1.4−10.8	2.8 ± 0.3
260	yes	1.94	15.1	1450	8	1.6−11.5	2.56 ± 0.12
280	no	1.90	15.0	1210	8	1.9−11.5	2.36 ± 0.07
299	yes	2.00	15.1	1620	8	0.9−12.4	2.35 ± 0.18
302	yes	1.93	15.1	1680	8	1.4−16.5	2.20 ± 0.03
304	no	2.01	14.9	1240	10	1.5−9.6	2.3 ± 0.2
330	no	1.32	8.0	1100	8	1.4−10.0	2.14 ± 0.05
330	no	1.91	14.9	1410	8	1.6−13.8	2.19 ± 0.06
330	no	3.90	29.6	1380	9	1.4−14.2	1.84 ± 0.09
360	no	2.03	15.0	1460	8	1.3−18.7	1.84 ± 0.09
360	no	2.06	15.0	1440	8	2.8−15.0	2.09 ± 0.11

[a] The indicated uncertainties in the *k* values represent the 95% confidence level of the fits of the k_m vs [NO] data, as in Figure 2.

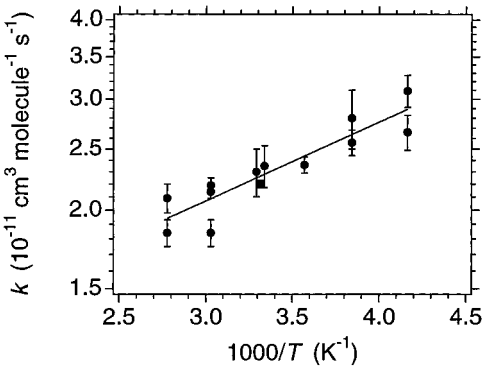

Figure 3. Arrhenius plot of the rate coefficient *k* for the CH_2=C-$(CH_3)C(O)O_2$ + NO reaction. Data taken with and without a Teflon tube inserted in the neutral flow tube are indicated by solid and open circles, respectively. The error bars shown are derived from the fits of the k_m vs [NO] data, as in Figure 2. The solid line shows the result of a fit of an exponential function to the experimental data. The rate coefficient is found to be $k(T) = 8.7 \times 10^{-12} \exp(290/T)$ cm^3 $molecule^{-1}$ s^{-1}, accurate within ±20% over the temperature range $T = 240-360$ K.

peroxy radicals.[10,11] This estimate is reasonable, as the measured wall loss on the injector increases to about 10 s^{-1} at 240 K, and the injector surface is much smaller than the reactor surface (reactor, 2.54 cm i.d.; injector, 0.64 cm o.d.). At these low temperatures, the radicals may tend to stick to or condense on the reactor wall to account for the increased wall losses.

A rate coefficient at 298 K of $(2.3 \pm 0.3) \times 10^{-11}$ cm^3 $molecule^{-1}$ s^{-1} has been determined from the measurements. This value is the average of the three measurements at room temperature, and the same value is calculated from the expression for $k(T)$ given above. The error bar represents the statistical uncertainty in the rate coefficient (at the 95% confidence level) plus a factor of 10% for possible systematic error.

Similar to the case of peroxyacetyl radical,[10] reaction 1 is expected to be followed by elimination of CO_2 from the acyl radical:

$$CH_2{=}C(CH_3)C(O)O \rightarrow CH_2{=}C{-}CH_3 + CO_2 \quad (11)$$

A search for the products of reactions 1 and 11 was undertaken but provided few definitive answers. As mentioned before, NO_2 is easily observable as a product of reaction 1, using the SF_6^- + NO_2 charge-transfer reaction. Detection of CH_2=$C(CH_3)$C-(O)O radicals is expected to be also possible using SF_6^-. Indeed, a small signal is seen at mass 85, corresponding to CH_2=$C(CH_3)C(O)O^-$ ions. The signal depends similarly to the PMA signal on the temperature of the quartz tube in the radical source, but if NO is added to the flow reactor, the signal decreases instead of increasing as a result of reaction 1. Most likely, the signal arises from unknown chemistry taking place inside the heated quartz tube, for example, from the methacrylic anhydride impurity in the MPAN sample, rather than from the product of reaction 1. The lifetime of the CH_2=$C(CH_3)C(O)O$ radicals in the neutral flow reactor may be too short to enable their observation. Detection of CH_2=$C-CH_3$ radicals, the products of reaction 11, is expected to be possible using O_2^+ ions. Indeed, a small signal is seen at mass 41, corresponding to CH_2=$C-CH_3^+$ ions, which depends similarly to the PMA signal on the quartz tube temperature. If NO is added, the signal increases, but this increase also occurs if the radical source is at room temperature, so the increase cannot be due to the PMA + NO reaction. Also, adding NO leads to a loss of O_2^+ ions inside the ion flow tube, as a result of the O_2^+ + NO charge-transfer reaction (5×10^{-10} cm^3 $molecule^{-1}$ s^{-1}).[17] For these reasons it is unclear whether the signal corresponding to CH_2=$C-CH_3^+$ ions is partly due to the formation of CH_2=C−CH_3 radicals as a result of reactions 1 and 11. It seems possible that the CH_2=$C-CH_3$ radicals also react with NO in the neutral flow tube to form CH_2=$C(CH_3)$NO. A final attempt to detect CH_2=$C-CH_3$ was made by adding an excess of O_2 to the neutral flow tube (up to half of the He was replaced by O_2), to quickly convert CH_2=$C-CH_3$ into CH_2=$C(CH_3)O_2$. This was done at small NO concentrations to minimize the CH_2=$C(CH_3)$-O_2 + NO reaction. It is expected that CH_2=$C(CH_3)O_2$ radicals can be detected using SF_6^-, but no ions were seen at mass 73, corresponding to CH_2=$C(CH_3)O_2^-$ ions.

4. Discussion

The conditions for measuring the rate coefficient for reaction 1 in the neutral flow reactor lead to a significant axial CH_2=C-$(CH_3)C(O)O_2$ radical concentration gradient. The possibility that the resulting forward diffusion of radicals influences the rate coefficient determination is investigated. The importance of forward diffusion can be estimated using[18]

$$k_c = k'(1 + k'D/v^2) \quad (12)$$

where k' is the measured first-order rate coefficient (s^{-1}), k_c the rate coefficient corrected for forward diffusion (s^{-1}), D the diffusion coefficient (cm^2 s^{-1}), and v the average flow velocity (cm s^{-1}). Using an estimate for the diffusion coefficient of PMA radicals in He of 75 cm^2 s^{-1} at 2 Torr and 300 K, the correction as a result of eq 12 is found to be a few percent at most. Since the correction is small and well within the experimental uncertainties in the present work, it is not applied to the reported results.

The rate coefficient of reaction 1 increases with decreasing temperatures, as expected for fast radical−radical reactions. Other experiments in our and other laboratories have demonstrated a similar behavior,[10,11,19,20] which is qualitatively explained by the formation of a bound reaction intermediate.

Villalta and Howard investigated the analogous $CH_3C(O)O_2$ + NO reaction using the same method as in the present work.[10] The rate coefficient was found to be $k(T) = (8.1 \pm 1.3) \times 10^{-12}$ exp{$(270 \pm 60)/T$} cm^3 molecule^{-1} s^{-1}, with a value at 298 K of $(2.0 \pm 0.3) \times 10^{-11}$ cm^3 molecule^{-1} s^{-1}. Maricq and Szente also studied the $CH_3C(O)O_2$ + NO reaction, using both transient IR absorption of NO and NO_2 and time-resolved UV spectroscopy of the $CH_3C(O)O_2$ radicals. Their results, $k(298\ K) = (1.4 \pm 0.2) \times 10^{-11}$ cm^3 molecule^{-1} s^{-1} and $E/R = -(570 \pm 140)$ K, differ significantly from those of Villalta and Howard. The reason for the discrepancy is not known, but the experimental method used by Maricq and Szente is less direct than that of Villalta and Howard. The presently reported rate coefficient for the $CH_2{=}C(CH_3)C(O)O_2$ + NO reaction agrees closely with the value for the $CH_3C(O)O_2$ + NO reaction as measured by Villalta and Howard. This suggests that, for $RC(O)O_2$ + NO reactions, the structure of an organic R group may have a minor influence on the rate coefficient. This observation is similar to the result of a study by Eberhard and Howard,[20] who found that the rate coefficient for RO_2 + NO reactions is nearly independent of the hydrocarbon group R, for R = CH_3, C_2H_5, *i*-C_3H_7, *n*-C_3H_7, $CH_2{=}CHCH_2$, *t*-C_4H_9, *c*-C_5H_9, and 2-C_5H_{11}. If supported by further studies, these findings imply that $RC(O)O_2$ radicals can be treated similarly, independent of the R group, in atmospheric models.

As described in the Introduction, the PMA + NO reaction plays an important role in the photooxidation of isoprene. Paulson and Seinfeld use a value of 1.4×10^{-11} cm^3 molecule^{-1} s^{-1}, independent of the temperature, for the rate coefficient of this reaction in their isoprene photooxidation model.[2] This value is somewhat smaller than the rate coefficient reported in this work. Carter and Atkinson use a room-temperature value of 2.25×10^{-11} cm^3 molecule^{-1} s^{-1} for the PMA + NO rate coefficient in their isoprene photooxidation mechanism.[3] This value and also the temperature dependence (though differently represented as $(T/300)^{-0.9}$) agree very well with the presently reported values. In smog chamber experiments, the Paulson and Seinfeld mechanism tends to underpredict ozone formation and NO oxidation in most cases, whereas the model by Carter and Atkinson performs better in this respect. It is not expected, however, that the rate coefficient of the PMA + NO reaction plays a major role in explaining the differences between the two models.

The question remains why the products of reactions 1 and 11 are not observed in the present study. Tuazon and Atkinson[6] studied the OH-initiated oxidation of methacrolein, $CH_2{=}C(CH_3)CHO$, in a smog chamber experiment at 298 ± 2 K and atmospheric pressure. They reported that about half of the OH reaction events involve addition to the double bond and about half involve abstraction of hydrogen from the −CHO group. The latter channel leads to the production of the PMA radical. In the presence of nitrogen oxides, NO and NO_2, products corresponding to the PMA radical undergoing reactions 1 and 2 are observed, namely, CO_2, from the decomposition of the $CH_2{=}C(CH_3)C(O)O$ product via reaction 11 and MPAN from reaction 2. They attempted to account for the fate of the other product of reaction 11, $CH_2{=}C{-}CH_3$, the methylvinyl radical, and considered two different routes. In both cases the first step is the addition of O_2:

$$CH_2{=}C{-}CH_3 + O_2 \rightarrow CH_2{=}C(CH_3)O_2 \qquad (13)$$

In one case the peroxy adduct undergoes an internal reaction via a four-center intermediate, analogous to the fate of the vinylperoxy radical. This intermediate decomposes to yield CH_2O and CH_3CO, with the latter product yielding the peroxyacetyl radical, $CH_3C(O)O_2$. In the second oxidation route, the $CH_2{=}C(CH_3)O_2$ radical is formed and reacts via a sequence of fast reactions with NO and O_2 to ultimately produce products such as CH_2O, CO_2, and $CH_3C(O)CHO$. In their study these products are not observed in amounts that are consistent with such a mechanism. Tuazon and Atkinson[6] concluded that the products formed in either of these schemes are not likely to be the fate of the $CH_2{=}C{-}CH_3$ radical and that the problem requires further study.

Another possible route for $CH_2{=}C{-}CH_3$ is an effective bimolecular reaction with O_2 to yield allene or methylacetylene:

$$CH_2{=}C{-}CH_3 + O_2 \rightarrow CH_2CCH_2 + HO_2 \qquad (14)$$

$$\rightarrow CHCCH_3 + HO_2 \qquad (15)$$

It is likely that these reactions would occur via the energetic peroxy adduct formed in (13). If one assumes that the C−H bond dissociation energy in propene to yield $CH_2{=}C{-}CH_3$ is the same as in ethylene,[21] $D_{298} = 111.2 \pm 0.8$ kcal mol^{-1}, the heat of formation of the $CH_2{=}C{-}CH_3$ radical can be estimated to be about 64 kcal mol^{-1}.[22] Using this figure, the $\Delta H_{r,298}$ for reactions 14 and 15 are estimated to be about −16 and −17 kcal mol^{-1}, respectively.[22] The formation of these products would also explain why no organic radical products are observed in our study.

The formation of allene or methylacetylene as intermediates in the atmospheric oxidation of the peroxymethacryl radical was recently tested in a chamber experiment by Atkinson and coworkers.[23] The setup was as described by Tuazon and Atkinson,[6] where the PMA radical was produced in the OH-initiated oxidation of methacrolein in the presence of NO and NO_2. No significant amount of allene or methylacetylene was detected,[23] so the formation and fate of the $CH_2{=}C{-}CH_3$ radical remain a mystery. More work is needed to study the products of reactions 1 and 11, to complete the photooxidation scheme of isoprene as described by Paulson and Seinfeld[2] and by Carter and Atkinson.[3]

Acknowledgment. The authors thank Dr. S. E. Bauerle for his assistance with the synthesis of MPAN and Dr. E. R. Lovejoy for useful help, discussions, and comments. This work is supported in part by the NOAA Climate and Global Change Program.

References and Notes

(1) Geron, C. D.; Guenther, A. B.; Pierce, T. E. *J. Geophys. Res.* **1994**, *99*, 12773.
(2) Paulson, S. E.; Seinfeld, J. H. *J. Geophys. Res.* **1992**, *97*, 20703.
(3) Carter, W. P. L.; Atkinson, R. *Int. J. Chem. Kinet.* **1996**, *28*, 497.
(4) Trainer, M.; Williams, E. J.; Parrish, D. D.; Buhr, M. P.; Allwine, E. J.; Westberg, H. H.; Fehsenfeld, F. C.; Liu, S. C. *Nature* **1987**, *329*, 705.
(5) Paulson, S. E.; Flagan, R. C.; Seinfeld, J. H. *Int. J. Chem. Kinet.* **1992**, *24*, 79.
(6) Tuazon, E. C.; Atkinson, R. *Int. J. Chem. Kinet.* **1990**, *22*, 591.
(7) Williams, J.; Roberts, J. M.; Fehsenfeld, F. C.; Bertman, S. B.; Buhr, M. P.; Goldan, P. D.; Hübler, G.; Kuster, W. C.; Ryerson, T. B.; Trainer, M.; Young, V. *Geophys. Res. Lett.* **1997**, *24*, 1099.

(8) Roberts, J. M.; Bertman, S. B. *Int. J. Chem. Kinet.* **1992**, *24*, 297.
(9) Maricq, M. M.; Szente, J. J. *J. Phys. Chem.* **1996**, *100*, 12380.
(10) Villalta, P. W.; Howard, C. J. *J. Phys. Chem.* **1996**, *100*, 13624.
(11) Villalta, P. W.; Huey, L. G.; Howard, C. J. *J. Phys. Chem*. **1995**, *99*, 12829.
(12) Bertman, S. B.; Roberts, J. M. *Geophys. Res. Lett.* **1991**, *18*, 1461.
(13) Seefeld, S.; Kinnison, D. J.; Kerr, J. A. *J. Phys. Chem. A* **1997**, *101*, 55.
(14) Huey, L. G.; Hanson, D. R.; Howard, C. J. *J. Phys. Chem*. **1995**, *99*, 5001.
(15) Madronich, S.; Calvert, J. G. *J. Geophys. Res.* **1990**, *95*, 5697.
(16) Moortgat, G.; Veyret, B.; Lesclaux, R. *J. Phys. Chem.* **1989**, *93*, 2362.
(17) Ikezoe, Y.; Matsuoka, S.; Takebe, M.; Viggiano, A. *Gas Phase Ion−Molecule Reaction Rate Constants Through 1986*; Mass Spectroscopy Society of Japan: Tokyo, 1987.
(18) Howard, C. J. *J. Phys. Chem*. **1979**, *83*, 3.
(19) Atkinson, R.; Baulch, D. L.; Cox, R. A.; Hampson, R. F.; Kerr, J. A.; Troe, J. *J. Phys. Chem. Ref. Data* **1992**, *21*, 1125.
(20) Eberhard, J.; Howard, C. J. *J. Phys. Chem. A* **1997**, *101*, 3360.
(21) Ervin, K. M.; Gronert, S.; Barlow, S. E.; Gilles, M. K.; Harrison, A. G.; Bierbaum, V. M.; DePuy, C. H.; Lineberger, W. C.; Ellison, G. B. *J. Am. Chem. Soc*. **1990**, *112*, 5750.
(22) Lias, S. G.; Bartmess, J. E.; Liebman, J. F.; Holmes, J. L.; Levin, R. D.; Mallard, W. G. *J. Phys. Chem. Ref. Data* **1988**, *17* (Suppl. No. 1).
(23) Atkinson, R. Private communication.